DØ Note 3563

LED Pulser System for the DØ Muon Upgrade Scintillation Counters

Pierrick Hanlet, Matthew Marcus, Darien Wood
Northeastern University, Boston, MA 02115
Al Ito, Bob Jones, Tom Regan
Fermi National Accelerator Laboratory, Batavia, IL 60510
B.S. Acharya
Tata Institute of Fundamental Research, Colaba, Mumbai 40005, India
Juan Pablo Negret, Manuel Zanabria
Universidad de los Andes, Bogota, Columbia

February 23, 1999

Abstract

We present the technical design for an LED based pulser system for the DØ Upgrade Muon Scintillation counters. For Run II, accurate timing information from the scintillation counters is imperative for the proper performance of the muon triggers. The LED Pulser System will serve in the commissioning of the counters and for the continuous monitoring of the PMTs' performances and gains.

A detailed description of the system is presented, as well as the results of tests on individual components and integrated system. Proceedures for production, assembly, quality control, installation, and commissioning are presented. Cost estimates and resource needs to complete the system are presented, as well as an estimated schedule.

From the test results, the DØ LED Pulser System performs at a level exceeding specifications for a fraction of the initial cost estimated for performing the required tasks.

DRAFT

Contents

1 Introduction **3**
- 1.1 Run IB Experience . . . 3
- 1.2 Motivation . . . 3
- 1.3 Specifications for an External Pulser System . . . 5

2 System Design **7**
- 2.1 The Scintillator LED Pulser . . . 8
- 2.2 The LED Driver Board . . . 9
- 2.3 LED Block . . . 10
- 2.4 Light Mixing . . . 11
- 2.5 Light Distribution . . . 12
- 2.6 Connection to PMTs . . . 15
- 2.7 LED Pulser System Monitoring . . . 15

3 Light Mixing and Pulser Stability Test Results **17**
- 3.1 LED Robustness . . . 17
- 3.2 LED Matching . . . 18
- 3.3 Light Mixing Uniformity . . . 19
- 3.4 Light Distribution to PMTs . . . 20
  - 3.4.1 Fiber Polishing . . . 20
  - 3.4.2 Tests on the Optical Fiber Coupling . . . 21
  - 3.4.3 Light Distribution Results . . . 22
- 3.5 LMB Stability . . . 22
- 3.6 PIN Diode Stability . . . 23
- 3.7 System Stability Against Voltage Fluctuations . . . 23
- 3.8 System Stability Against Temperature Fluctuations . . . 23

4 System Control **25**

5 Component List and Cost Estimate **26**

6 Manpower Requirements **28**

7 Production, Installation, and Commissioning **29**
- 7.1 LMB Production . . . 29
- 7.2 LMB Testing . . . 29
- 7.3 LMB Installation and Fiber Routing . . . 29
- 7.4 System Integration . . . 29

8 Procurement and Schedule **30**

9 Conclusion **32**

DRAFT

1 Introduction

We present a design for the LED Pulser System for the muon upgrade scintillation counters. The purpose of this pulser system is to provide means for testing, commissioning, calibrating, and monitoring the counters gains and timings. The system described is based on a modified version of what was successfully used by the E760 collaboration for monitoring their electromagnetic calorimeter photomultiplier tubes, or *PMTs*[1].

The Run II muon system, described in detail in other documents[2], contains three sets of scintillation counters. The central pseudo-rapidity region covers the range ($|\eta| \lesssim 1$); it consists of the C-layer "Cosmic Cap" and "Bottom", B-layer "Side", and A-layer "$A\phi$" counters, or *CMSC* counters. The forward region covers ($1 \lesssim |\eta| \lesssim 2$) has six—3 north and 3 south—planes of pixel counters, or *FMSC* counters, in an η–ϕ geometry. The number of counters in each system is given in Tables 1 and 2. The Cosmic Cap was installed and operated in Run IB and are described in [3].

1.1 Run IB Experience

Our experience during Run IB with the 240 counters of the Cosmic Cap guides us to design and install a calibration system with an external light source. The method used during Run IB was to commission the counters with cosmic ray muons, then set and fine-tune the timing gate using beam muons. The latter was accomplished over a period of approximately 4 months (for each octant of counters as they were installed); eventually the gate was narrowed from 500ns to 50ns width. In addition, the gain of the PMTs changed during the course of the run due to burn-in of new tubes and slow, long-term aging due to integrated anode current. Furthermore, we required occasional threshold adjustments to discriminator thresholds, since groups of PMTs shared a common high voltage channel.

Some of the techniques we used during Run IB will not be applicable to the Run II muon system. For instance, we indirectly monitored the gain using the coincidence rate for both PMTs on each Cosmic Cap counter, to eliminate the rate of tube noise from the estimate. This will not be possible in the $A\phi$ and FMSC counters which have one PMT per counter.

The procedure of using beam muons to check the timing and gain calibrations was a long process which resulted in delayed turn on of the scintillator system. Given an order of magnitude more counters and tighter timing requirements in the upgrade detector, it will be considerably more difficult to use beam muons to perform and maintain the calibration in Run II.

1.2 Motivation

For commissioning of the detector, we would like to have a means of setting PMT gains in situ. In addition, we would like to have a means to measure relative timing differences between counters so as to be able to adjust trim cables in situ, *before roll–in*. Afterwards, with all counters relatively timed, we will be in a position to promptly determine the absolute timing of the scintillator systems with beam, which in turn will allow for prompt timing in of the WAMUS and FAMUS chambers with cosmic muons.

During the run, we would like to have a means for performing the following tests and calibration on short notice which could immediately yield numerous results. With an LED pulser system:

1. it is trivial to find dead PMTs quickly,
2. we can isolate the behavior of the PMTs from the front end electronics,
3. we can find and adjust relative timing between channels due to variations in PMTs,
4. we can use early timing of scintillator counters to immediately time in PDTs and MDTs,
5. we can use the LED Pulser to set initial PMT gains,

6. we can monitor PMT gains,

7. we can track timing changes with threshold and voltage changes.

We have considered a variety of methods for monitoring the timing and gain calibrations during Run II. The best alternative appears to be the use of beam muons to perform the task, as we did in Run IB for the Cosmic Cap. In what follows, we estimate the required time to perform such a calibration for Run II FMSC counters: The system timing for the trigger is $\sim$ 5ns. To calibrate the timing to 0.5ns requires 100 muons per counter, which in turn requires muons with $p_T > 3$ GeV and readout of some large fraction of the detector. At $\mathcal{L} = 1 \times 10^{32}\text{cm}^{-2}\text{s}^{-1}$, this single muon rate is $\mathcal{O}(50)$Hz. Since each muon will cross 3 counters, we require 100 muons/(3 counters) $\times$ 4500 counters $= 1.5 \times 10^5$ muons. Assuming a 50% background, we require 3×10^5 muons. Thus, assuming a DAQ rate of $\mathcal{O}(10)$Hz, we will require an $\sim$8hr dedicated run for enough backgroundless muons to perform the calibration. The gain calibrations require 16$\times$ as many muons because of the multiplexing of the ADC readout. Though this is not an inordinate amount of time, the learning curve and subsequent reconstruction and muon identification would require on the order of several weeks time scale at best. This long time-lag would severely impair detector monitoring and debugging.

It will still be necessary to check the timings and gains of the scintillators with beam muons, which will ultimately yield the absolute calibration corrections. If the relative differences of the counters can be removed via use of the LED Pulser System, then the data from many counters can be combined, and more precise offline calibrations can be obtained more quickly. In short, with the LED Pulser System we expect to be taking physics quality data much earlier than without it.

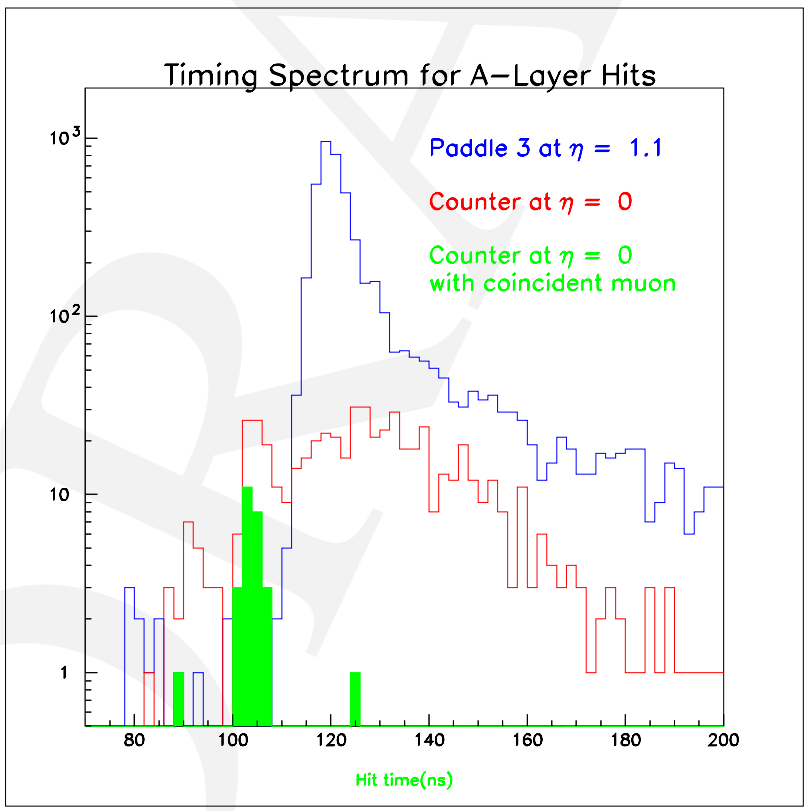

Figure 1: Run I Muon Stub Time Spectrum

For Run II, hits in the muon scintillation counters will be used in the trigger to reject out–of–time

muons. This implies the correct timing of muon signals is imperative to the operation of the muon trigger. This can be seen in Fig. 1, which shows the time spectrum for hits in muon scintillation test counters placed in the A–layer at $\eta = 0$ and $\eta = 1.1$ during Run I. In the figure, for the counter at $\eta = 0$, one sees a large background of out–of–time muons in red, and a clear in–time muon signal in green.

Fig. 2 shows a cartoon of how a change in the PMT gain—shown as ΔV— translates to a signal timing change Δt; e.g. for a 10 ns risetime, a 10% gain change would correspond to a 1 ns signal timing drift. The LED Pulser System will serve to continuously monitor PMT gains so as to flag counters which fall out of tolerance. Since all PMT signals have a risetime of < 10 ns, the monitoring the gains to a 10% level will insure proper timing of all counters for the muon trigger.

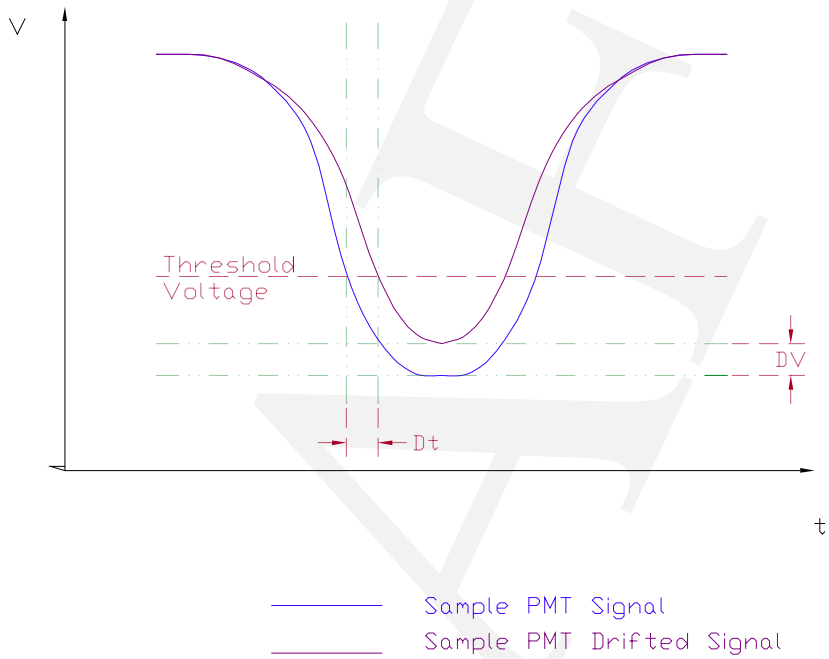

Figure 2: Example of how the trigger timing changes with PMT gain change

1.3 Specifications for an External Pulser System

The following are the requirements for an external light calibration system:

- a short duration light pulse with < 10 ns rise time,
- a fall time of ~ 50 ns,
- a variable amplitude signal in the MIP range,
- a variable delay capability,
- a 200Hz rate capability,
- a distribution of the light pulse to each scintillation counter,
- a control capability directed by the DØ data-acquisition and controls system.
- match of emission spectrum of LED and wavelength shifting fibers(bars) in the central(forward) region

In what follows, we present the details of a system which meet the above specifications. We start by describing the six major components of the calibration system. This is followed by test results of uniformity and stability, system control, a presentation of the component count for the CMSC and the FMSC counters, installation and commissioning, manpower requirements, schedule, and conclusions.

DRAFT

2 System Design

The LED Pulser System will be an integral part of the DØ Online and Data Acquisition systems, with all of the necessary control, monitoring, and analysis capabilities.

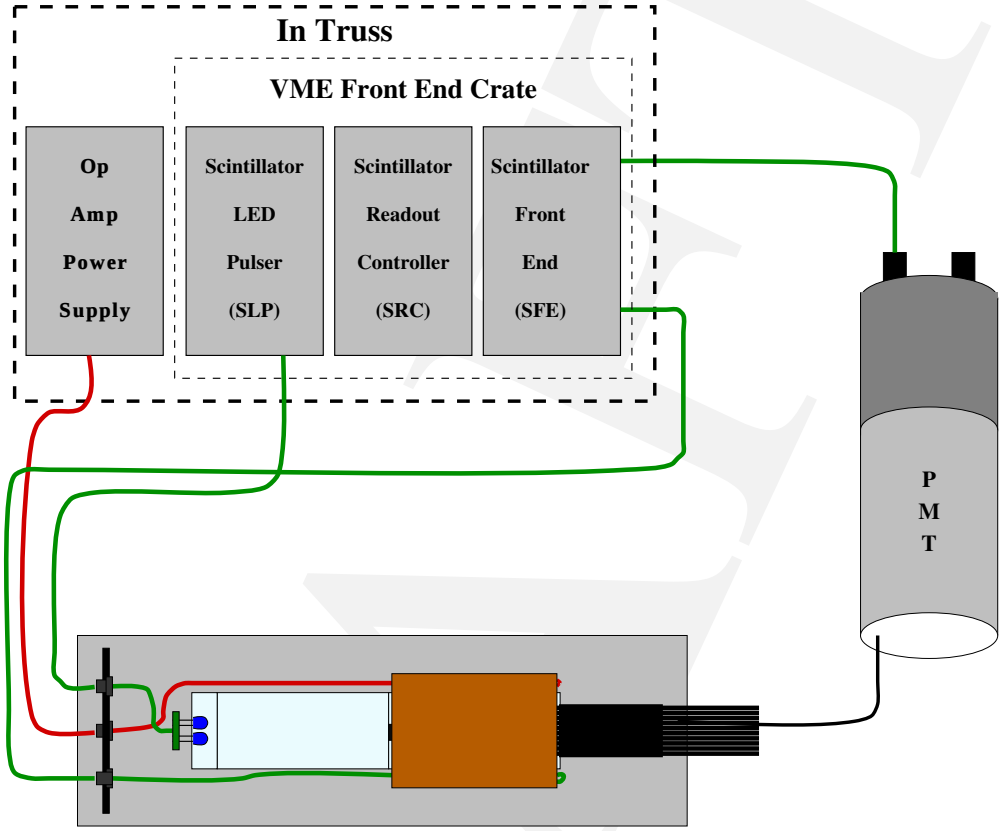

Figure 3: Block Diagram of LED Pulser System for single channel

The LED Pulser System consists of seven major components, listed below. The first six have been prototyped and are being tested. The reader is referred to [4] for a detailed description of the muon readout system.

1. Scintillator LED Pulser, *(SLP)*
2. LED Driver Board, *(LDB)*
3. LED Block
4. Light Mixing
5. Light Distribution *(Fiber Block)*
6. System Monitoring *PIN Diode/Amplifier*
7. Readout

An example of the scintillator calibration and monitoring system for one channel is shown in Fig. 3. In the figure, the Scintillator LED Pulser, or *SLP*, generates a pulse to trigger the LED Driver Board, or *LDB*, which drives the LEDs in the LED block. The light is then mixed in two lucite mixing blocks

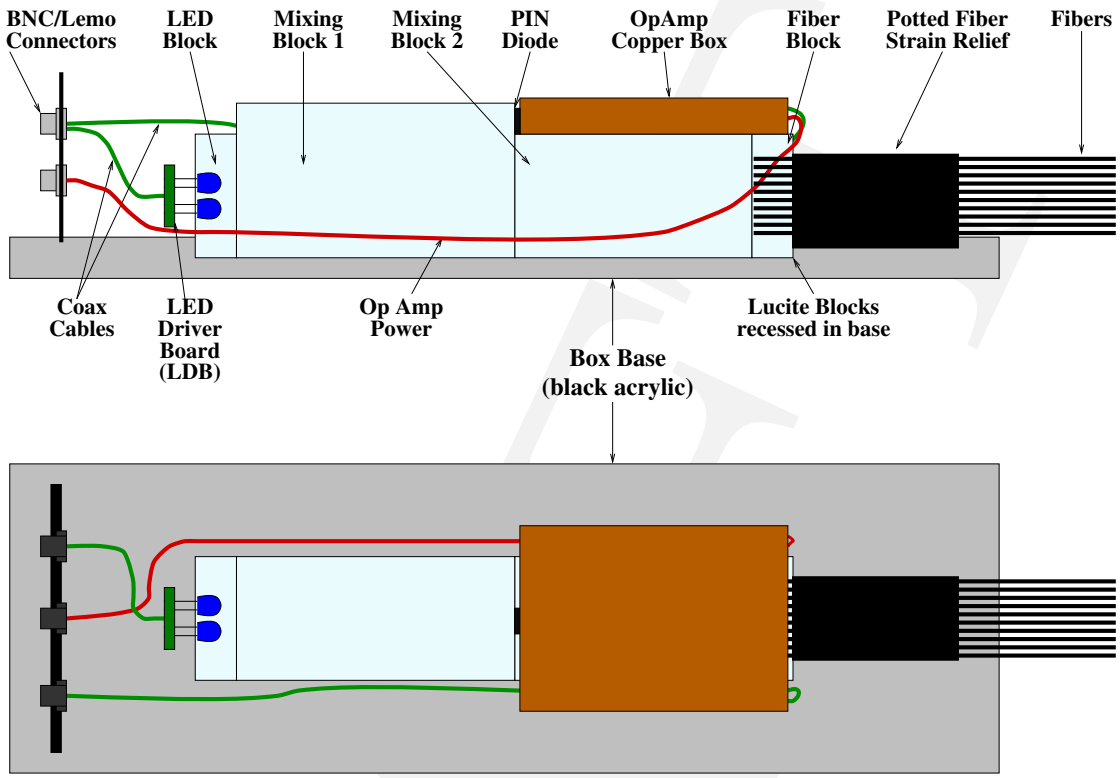

Figure 4: Light Mixing Block

and is distributed to individual PMTs via fiber optic cable. The mixed light to the PMTs is monitored using a PIN Diode which is located downstream of the first mixing block; this signal is amplified using an OpAmp circuit and line driver. The LDB, LED Block, Mixing Blocks, and Fiber Block are all housed in the Light Mixing Box, or *LMB*, as shown in Fig. 4. Both the PMT signal and OpAmp signal are read out using standard Scintillator Front End, *SFE*, readout cards[5].

2.1 The Scintillator LED Pulser

The Scintillator LED Pulser[6], *SLP*, is a custom $9U \times 280$ mm VME board which has been designed by Tom Regan. There will be one SLP in each scintillator front-end crate. A block diagram of the SLP is shown in Fig. 5. The Scintillator Readout Controller, *SRC*, in the same crate communicates with the SLP via the VME backplane.

The SLP performs the following functions:

- Accepts VME back plane trigger
- Accepts an LVDS—Low Voltage Digital Signal—test pulse trigger from the SRC via the backplane.
- Accepts NIM external test pulse input Lemo from front panel
- Accepts front panel push button trigger
- Allows VME controlled channel enable
- Allows VME controlled channel amplitude control

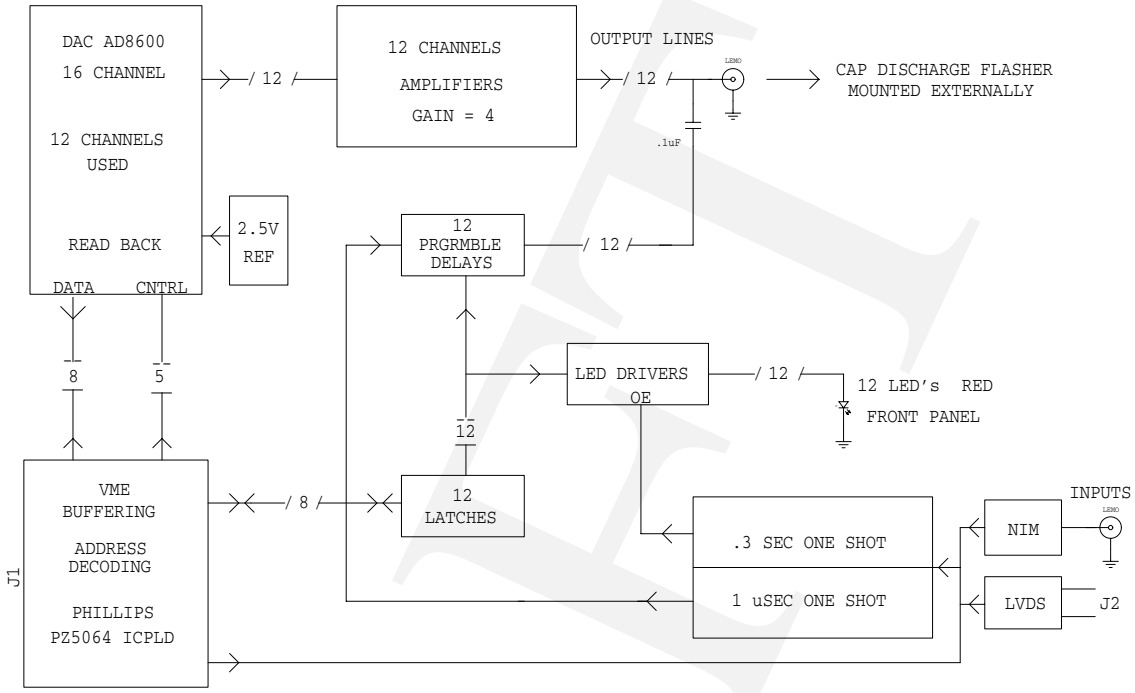

Figure 5: Block Diagram of the SLP

- Allows VME controlled individual channel delay
- Outputs each of 12 channel's LED driver signal via front panel BNC
- Flashes front panel display LED when channel is output

The SLP outputs 12 channels of a DC offset TTL signal; each channel is enabled by a VME controlled 12–bit R/W channel enable register. The DC offset for each channel is set by the VME controlled 8–bit R/W DAC and is limited to a 2.5 V maximum output. The DAC output is then amplified by a $\times 4$ opamp and added resistively to the TTL signal, yielding a 10 V maximum output. The variable delay of each channel is set by a VME controlled R/W register which controlls two programmable delay lines of 8 20ns steps and 16 2ns steps. Each channel is designed to have an amplitude stability of $< 1\%$ and a channel–to–channel time skew of < 1 ns.

2.2 The LED Driver Board

The LED Driver Board, Fig. 6, delivers a negative going differentiated pulse to each of the four LEDs in an LED block. The circuit operates by charging and subsequently discharging a capacitor when a TTL trigger pulse is received from the SLP module. The pulse amplitude is determined by the DC offset of the SLP output. The leading edge rise time is designed to be < 8 ns. The trailing edge fall time is controlled by values of RC and is selcted to have a $\sim$30 ns time constant. This pulse shape was designed to best match a MIP signal from muons in Pixel, A–ϕ, and CMSC counters while still using only one LDB design. For the blue LEDs, Sec. 2.3, the capacitor value was chosen to be 330 pF; for the bluish-green LEDs the capacitor value will be 390 pF.

The LDB is located inside the LMB box and is soldered directly to the LEDs in the LED block. The input signal is transported from the SLP to the LMB via RG58-U coaxial cable. Within the box, the SLP signal is fed through a BNC/lemo bulkhead connector, and on to the LDB via RG174-U coaxial cable.

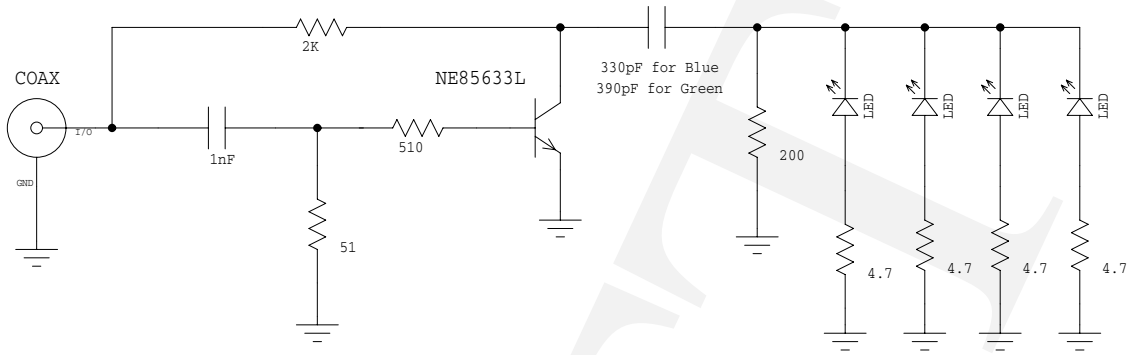

Figure 6: LED Driver Board: LDB

In order to ensure that the manufacturer specified current limit for the LEDs is not violated, a current limiting resistor is place on each LED leg of the circuit. The current limiting resistor value of $R = 5.1\Omega$ is chosen such that at the maximum SLP output of 10 V, each LED will have a maximum current of < 100 mA.

2.3 LED Block

An LED block is a lucite block with four LEDs potted in the block. The dimensions and LED positions are shown in Fig. 7. Since the drilling proceedure for the LED holes can sometimes cause crazing in the lucite, the blocks are annealed at 230 degF for 3 hours to insure that the blocks will not crack in time.

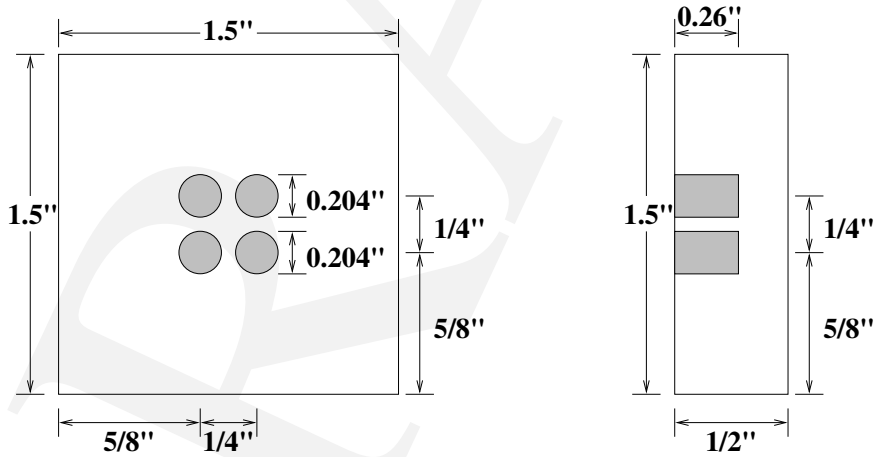

Figure 7: LED Block Dimensions

Four LEDs are potted in the LED block. In order to ensure the relative stability and uniform luminosity of the LEDs within an LED Block, the LEDs are prematched to draw a balanced current load between the four legs of the LDB circuit while delivering similar luminosities.

The LEDs are potted in an acrylic block using General Electric's RTV 615A Silicone Rubber Compound. Since the design is to distribute the light to the PMTs uniformly, the potting acts to remove the lensing effect of the LED casing by taking advantage of the similar indices of refraction of the LED casing, glue, and lucite.

Two types of LED blocks are used in the system, each differentiated by the type of LED potted in the block. In the central region, Blue-Green NSPE510S LEDs from Nichia America Corporation are chosen

since the peak wavelength and shape of their emission spectrum best matches that of the wavelength shifting fibers used in the counters, Fig. 8(a). In the forward regions, Blue NSPB320BS LEDs from Nichia America Corporation are used since the peak wavelength and shape emission spectrum best matches that of the wavelength shifting bar used in the pixel counters, Fig. 8(b).

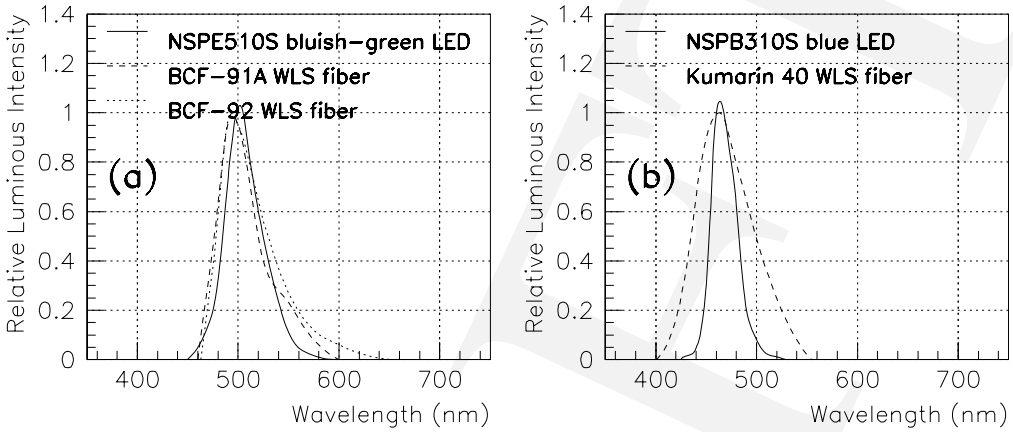

Figure 8: Emission Spectra for WLS fibers, bar, blue LEDs, and blue–green LEDs

2.4 Light Mixing

The light is further mixed in two additional lucite mixing blocks. The upstream side of each block is frosted by sand-blasting the lucite with a high powered silica bead blaster. The sides of the block are polished to maximize total internal reflection within the remainder of the block.

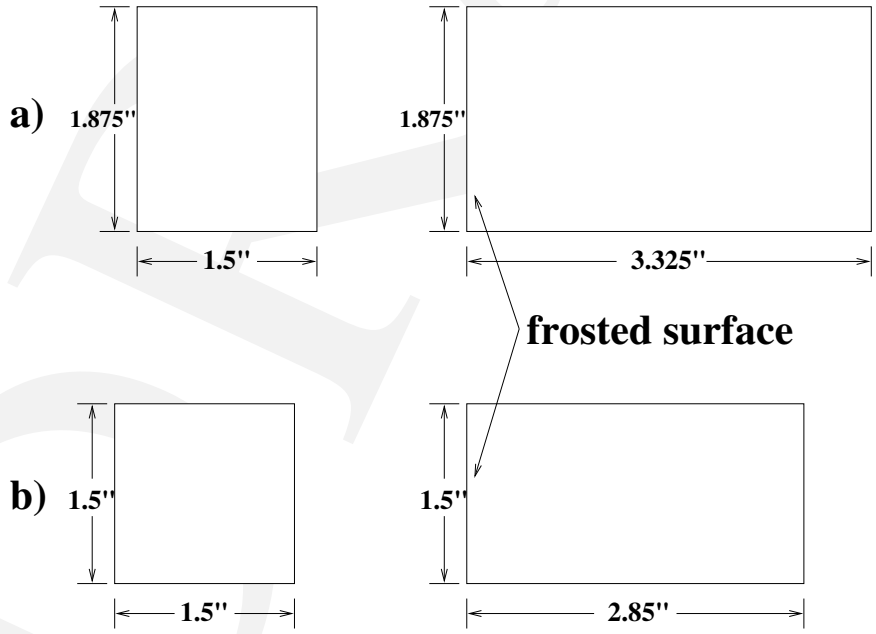

Figure 9: Mixing Block Dimensions: a) is first (upstream) mixing block, b) is second (downstream) mixing block

The first mixing block is used both to mix the light, to physically separate the PIN diode/OpAmp from signals induced by the LDB pulses, and to provide a surface from which the PIN diode can collect light. Dimensions of the blocks are shown in Fig. 9. Note that the first mixing block is larger than the second mixing block by $3/8''$ in one transverse dimension so as to accommodate the PIN diode. The second mixing block is square in cross section and serves to further mix the light using total internal reflection and by taking advantage of the optimal aspect ratio of $length = 1.9 \times width$[7]. Both mixing blocks are polished using a diamond polishing wheel.

Mixing Block Construction

The construction of the mixing blocks is performed in the steps:

1. rough cut blocks
2. polish one end of block
3. sand blast polished end
4. polish remaining sides

Care must be taken to avoid touching frosted surface. When complete, the blocks are wrapped in a soft cover for protection from scratches.

2.5 Light Distribution

Each LMB serves to pulse numerous PMTs by distributing the mixed light to individual PMTs via Hewlett Packard HFBR-500 clear optical fiber cable. A lucite block, into which these fibers are glued, has the same transverse dimensions as the second mixing block, as shown in Fig. 10. This block, with fibers inserted, is referred to as the *fiber block*. Within each fiber block, the length of each fiber is identintical.

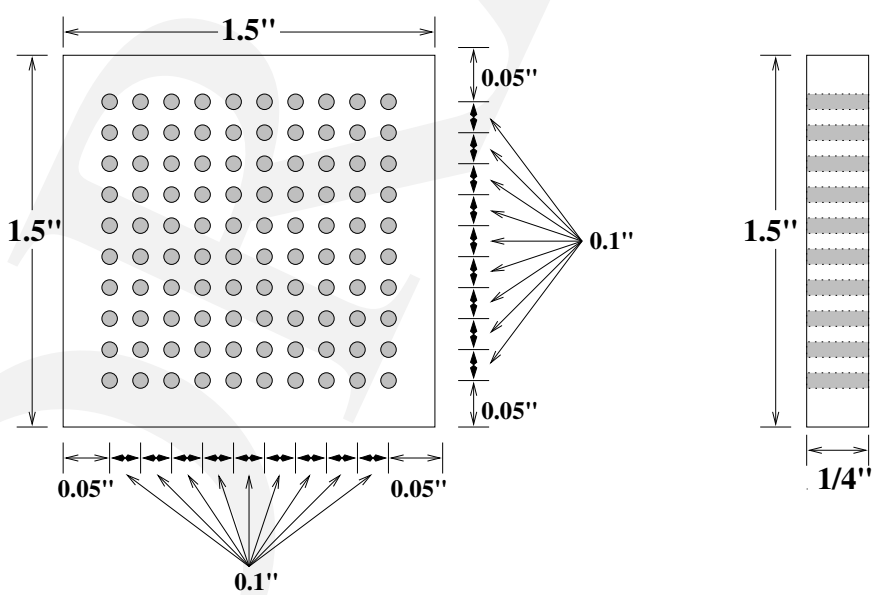

Figure 10: Fiber Block Dimensions

In order to minimize the cost of the project, it is important to reduce the amount of optical fiber used. We have managed to do so by minimizing both the number of fibers in each LMB and the length of the fibers. Minimizing the number of fibers in an LMB is accomplished by using arrays of 4×4, 4×5, 5×5, 7×7, 7×8, or 10×10 fibers in a block. In doing so, we must also simultaneously optimize:

1. fiber lengths minimized
2. fibers reach as many counters as possible
3. fiber length $\leq$5 m
4. radius of curvature for the fibers $\geq$35 mm
5. a minimum of 5% spare fibers in each block

In order to insure the safety of the fibers while still maximizing the number of fibers out of each LMB, the LMB is restricted to serve counters mounted together, such that:

- fibers never cross from one piece of iron to another,
- fibers never cross from one octant to another,
- fibers never cross over PDTs which have independent mountings.

Fiber Block Construction

The construction of the blank fiber block is performed in the steps:

1. cut fiber block to size $1.5'' \times 1.5'' \times 1/4''$—polishing not required
2. precision drill arrays of 10×10—$0.040''$ through holes separated by $0.095''$

The fibers are be prepared and inserted into the blank fiber block using the following proceedure:

1. cuts fibers to length
2. strip one of of the fiber with special stripper on shortest stop setting
3. apply RTV $\sim$1 cm from stripped end
4. dip stripped end of fiber into premade Bicron 600A epoxy
5. insert fiber into connector using twisting motion to spread glue and RTV being careful that $\sim$1–2 mm of fiber protrudes from the connector
6. crimp connector and spread excess RTV around the back of the connector
7. let glue and RTV set
8. polish fiber in modified Fiberfin III polisher
9. inspect polished end with magnifying glass
10. reject fiber if gouged, cover fiber if OK
11. strip unconnected end of fiber 3/8 in
12. dip stripped fiber in epoxy

13. insert stripped fibers into hole and twist to distribute epoxy
14. set epoxy with sheathed fiber ends held normal to lucite block face
15. fill region between fibers with carbon filled epoxy—this provides light tightness between the fibers
16. polish fiber block face with diamond polisher
17. cover lucite block end with soft cloth for protection

For each sub–detector section of the muon system, the number of counters, number of PMTs, and required type and number of LMBs are given in Tables 1 and 2, for central and forward regions respectively. Due to the variety of counter types in the central region, a total of 36 LMBs of each flavor is required to serve the 1,326 PMTs. In the forward regions, a single 10×10 LMB is required for each octant; a total of 48 LMBs to serve 4608 PMTs.

CMSC								
Octant	Region Layer	Iron	Counters/ Octant	Counters	PMTs	LMB Type	LMB #	Fiber Length(m)
0,1,2,3,4,7	A	CF	90	540	540	10×10	6	5.5
5,6	A	CF	45	90	90	7×7	2	5.0
4,7	B	CF	6	12	24	4×4	2	4.0
5,6	B	CF	20	40	80	7×7	2	4.0
0,1,2,3,4,7	C	CF	24	144	288	7×8	6	5.0
5,6	B	N-EF	8	16	32	4×5	2	2.0
4,7	B/C	N-EF	9	18	36	5×5	2	3.5
0,1,2,3	C	N-EF	8	16	64	4×5	4	2.5
5,6	B	S-EF	8	16	32	4×5	2	2.0
4,7	B/C	S-EF	9	18	36	5×5	2	3.5
0,1,2,3	C	S-EF	8	16	64	4×5	4	2.5

Table 1: Types and distribution of LMB's for the central Muon Scintillator System

FMSC								
Octant	Region Layer	Iron	Counters/ Octant	Counters	PMTs	LMB Type	LMB #	Fiber Length(m)
0-7	A	N-EF	96	768	768	10×10	8	4.20
0-7	B	N-EF	96	768	768	10×10	8	3.25
0-7	C	N-EF	96	768	768	10×10	8	3.25
0-7	A	S-EF	96	768	768	10×10	8	4.20
0-7	B	S-EF	96	768	768	10×10	8	3.25
0-7	C	S-EF	96	768	768	10×10	8	3.25

Table 2: Types and distribution of LMB's for the forward Muon Scintillator System

2.6 Connection to PMTs

At the end of each fiber from a fiber block is a Hewlett Packard HFBR-4501B black simplex connector. Butted up to each PMT is a polished piece of fiber with the black simplex connector on the other end; the connector end of the fiber is then plugged into a black bulkhead connector, Hewlett Packard HFBR-4505B. Coupling between the LMB fibers and PMT fibers is made with the bulkhead connector.

In the CMSC system, the unconnected fiber end is drilled and glued into a lucite cookie which holds all other fibers from the scintillator; the other end of the fiber is connected to a bulkhead connector in the counter top hat. In the FMSC system, 87 mm fibers with polished end are taped to the wave–length shifting bars which mate to the PMTs; the other end of the fiber is fed through a hole, which is subsequently filled with RTV, and coupled to a bulkhead connector mounted on the counter chasis.

In the FMSC counters, light transmission variations of $\pm 7\%$ were observed in the fibers between the PMTs and bulkhead connectors. Since the difference between FMSC and CMSC pieces are minimal, the same variations in light transmission are expected in the CMSC system.

2.7 LED Pulser System Monitoring

The bench tests of mixing blocks show that the light is disbributed homogeneously to the fibers (see Sec. 3.3). Consequently, we can monitor the light with a PIN diode at the downstream end of the first mixing block, and use this to track the light intensity for all of the fibers in the LMB over extended time periods.

The idea behind monitoring the light output is that the variations in the LEDs over time can be corrected by taking the ratio of the LED light measured by the PIN diode, $\mathcal{A}_{PIN}$, at present time t to initial time t_0. This correction factor is applied to the PMT response to LED pulses, $\mathcal{A}_{PMT}(t)$.

Using LED pulses, the fractional change in PMT gain, $\mathcal{F}_{\mathcal{A}}$ is given by the ratio of the difference in corrected PMT amplitudes to the PMT amplitude at t_0:

$$\mathcal{F}_{\mathcal{A}} = \frac{\mathcal{A}_{PMT}(t) \times \frac{\mathcal{A}_{PIN}(t_0)}{\mathcal{A}_{PIN}(t)} - \mathcal{A}_{PMT}(t_0)}{\mathcal{A}_{PMT}(t_0)} = \frac{\mathcal{A}_{PMT}(t)}{\mathcal{A}_{PMT}(t_0)} \times \frac{\mathcal{A}_{PIN}(t_0)}{\mathcal{A}_{PIN}(t)} - 1 \tag{1}$$

When 10% or larger variations in PMT gains are observed, the online system will notify the users so that action may be taken.

PIN Diode and Amplifier

We are using a Hamamatsu S6775 Silicon PIN photodiode. The photodiode is operated at a reverse voltage of 6 V and the output current is converted and amplified by a charge sensitive preamplifier, *CSP* Fig 11, taken from the Muon electronics used for Run 1. The output from the CSP is amplified by a factor of 40 by a OPA650 operational amplifier and a MAX435 transconductor. The combined system, Fig. 12, converts 70k photons, or a 7.1 fC signal, from the photodiode to a 100mV output signal at the amplifier. The power requirements are 7 mA at -12V and 12 mA at +6V for a total of 156 mW.

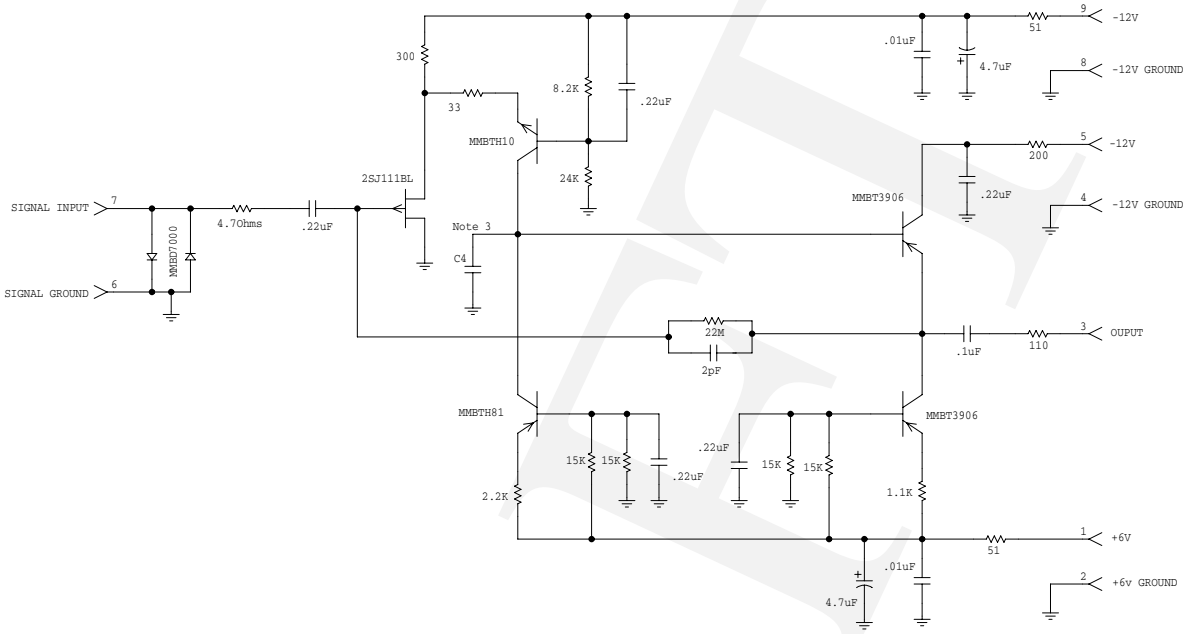

Figure 11: D0 Charge Sensitive Preamp: CSP

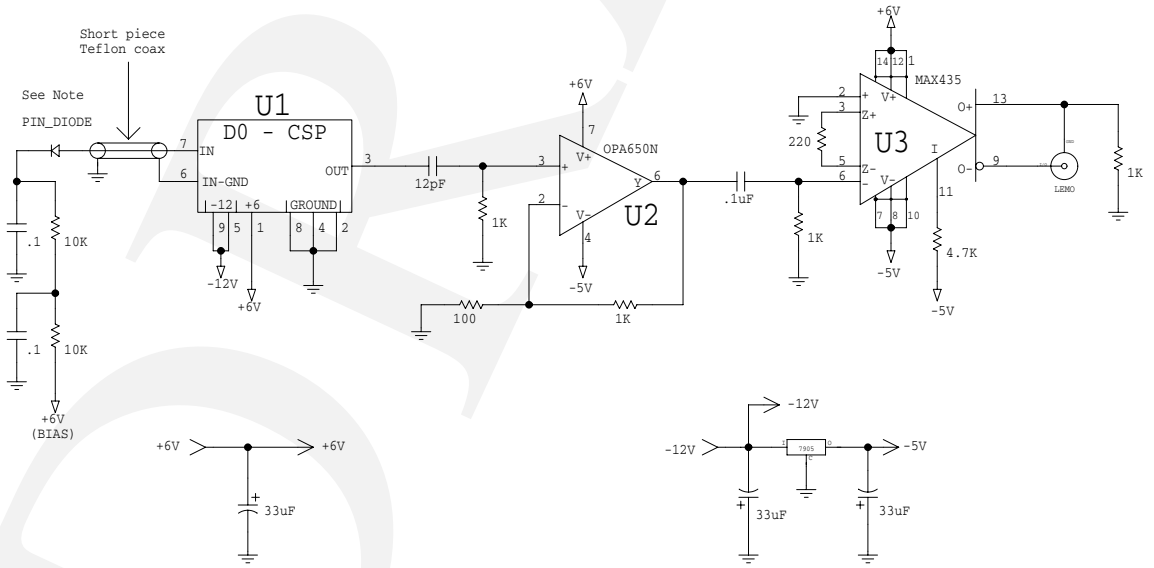

Figure 12: Amplifier Circuit Diagram for PIN Diode

3 Light Mixing and Pulser Stability Test Results

3.1 LED Robustness

A primary concern for light mixing is that all 4 LED's in an LED Block yield the same luminosity, $\mathcal{L}$, to within 10%. Since LEDs are inherently non-linear devices, it is equally important that the luminosity is attained by driving all four LEDs with the same current. This spurs an interest in the long term stability of the LEDs to insure that they do not change characteristics over time or integrated current. A second concern is that if the LEDs are matched at one point in their $\mathcal{L}$—vs—V or $\mathcal{L}$—vs—I curves, will they still be matched at another operating point?

We expect to operate the LMB at frequencies $\mathcal{O}$(1 Hz). Therefore to observe the LED's behavior over the course of Run II, we pulsed a single LED with 30 mA pulses with a duration of 30 ns at a rate of 1.5 kHz for 5,283 minutes (3.7 days). This corresponds to about 5× longer than a predicted 3 year run, and is equivalent to a total integrated current of 0.014 C. The luminosity vs time dependence was measured by setting the driving voltage of the SLP such that the LED yielded a specified amount of light as measured by the PIN diode. Using the voltage drop across an LED–resistor leg as a measure of the change in luminosity, the long term stability of the LED is shown in Fig. 13.

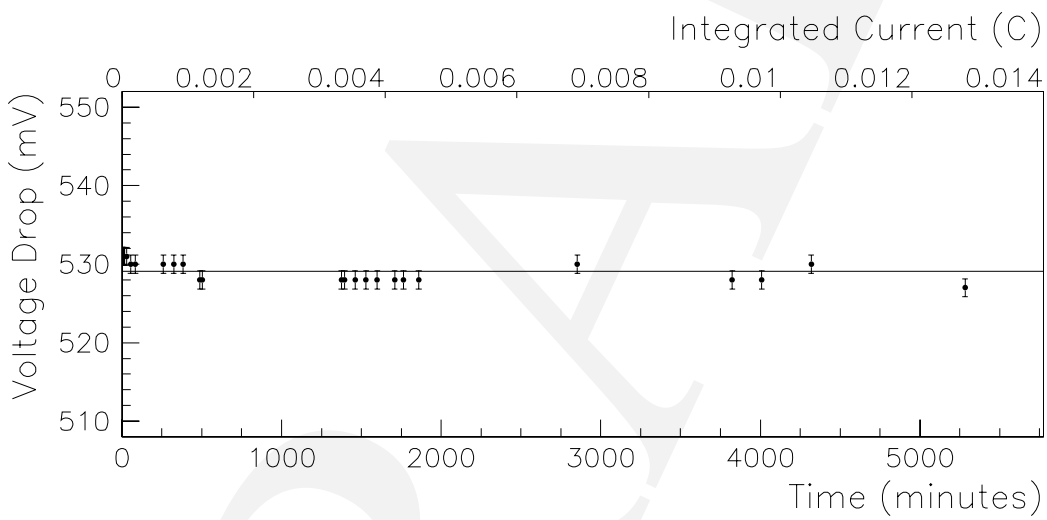

Figure 13: LED Luminosity vs Time and Integrated Current

The voltage required to drive at the reference luminosity fluctuated ±0.02 V (±0.4%) through out the study. Considering the measurement errors, the luminosity variations of the LED are consistent with a stable LED for the integrated current used in our measurement.

In addition, our tests show that the Nichia LED's do not have a burn in period.

LED Current Limitations

According to the manufacturer specifications, Nichia LEDs should not be driven with currents larger than 100 mA. Currents exceeding the manufacturer's specifications can have two possible effects on the LED. The first being that the LED will cease to operate; the second is that the high current may change the LED's characteristics, such as the luminosity voltage dependence.

In the event of a malfunction in the circuit in which the current may reach a level that exceeds the Nichea's specifications, tests were performed to push the limits. Pulsing a single LED at 1.5 kHz with currents up to 188 mA revealed that the LED did not die and the $\mathcal{L}$—vs—V dependance did not change.

Additional tests were made to measure the current through a single LED leg in the LDB. Even with the SLP driving at 10 V, the current through any LED was < 50 mA. We conclude that even if the SLP and LDB circuits malfunction, the LEDs will not fail from being operated out of the range of the manufacturer's specifications.

3.2 LED Matching

As previously mentioned, LEDs are prematched before being potted into the LED block. To verify that matching the LEDs at one point along the $\mathcal{L}$—vs—V curve would not result in mis–matched LEDs operated at another point, 3 bluish–green and 3 blue *unmatched* LEDs $\mathcal{L}$—vs—V curves were measured as shown in Fig. 14. In the figure, different polymarkers represent different LEDs.

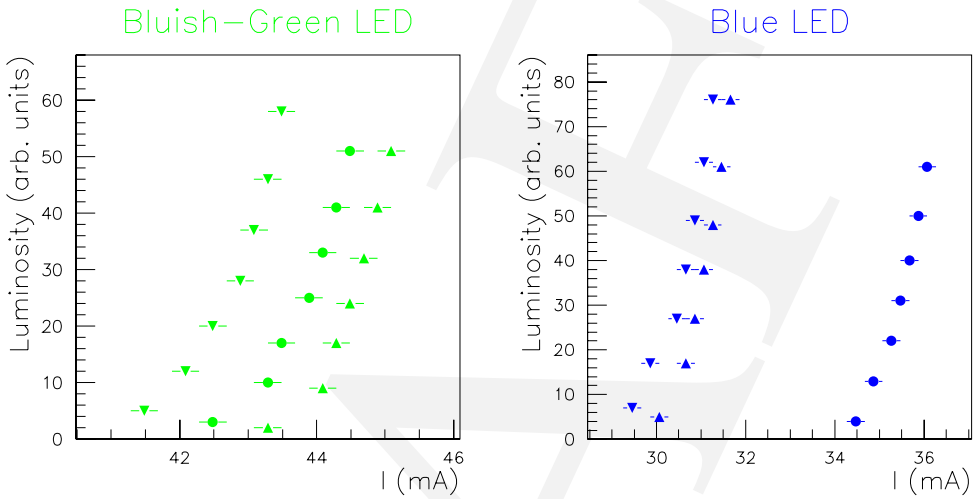

Figure 14: $\mathcal{L}$—vs—I curves for Nichea bluish–green and blue LEDs

To better see whether the LEDs match, the lower current curves in Fig. 14 were scaled by current to match the higher current curve in each plot and replotted in Fig. 15. In these plots unmatched LEDs are used. Hence, one can predict that as long as matched LEDs are operated within a stable region, i.e. high enough on the $\mathcal{L}$—vs—V curve, that they will remain matched over the range of operation.

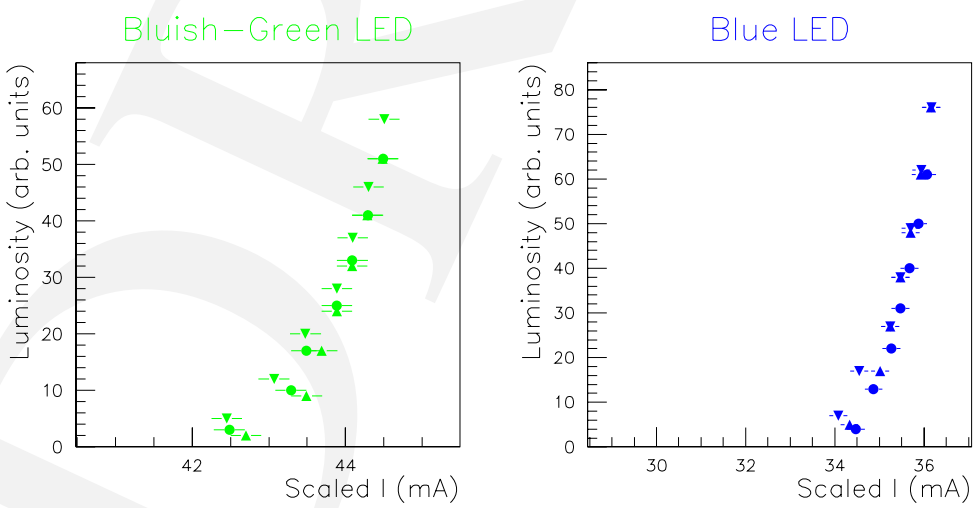

Figure 15: $\mathcal{L}$—vs—I curves with currents scaled for Nichea bluish–green and blue LEDs

3.3 Light Mixing Uniformity

In order to study how homogeneously the light is mixed in the combination of LED block, first and second mixing blocks, a blank fiber block was mounted in the LMB box. In each of the 100 holes of the blank fiber block, a fiber which was attached to a PMT was inserted. For each point both the PMT and PIN Diode outputs were recored using a LeCroy 3001 qVt in integrated charge mode. Fig 16 shows the

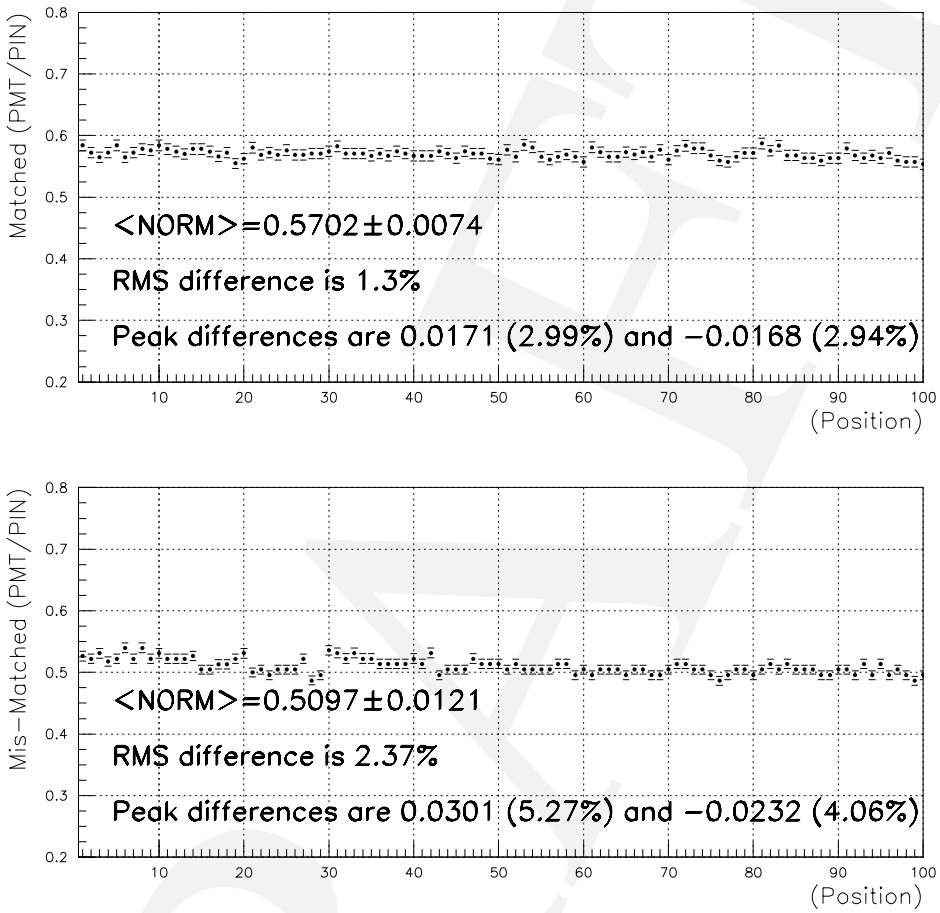

Figure 16: LMB Light Mixing Uniformity after the LED block and two mixing blocks: the top plot uses matched LEDs, the bottom uses mis–matched LEDs in the LED block

peak ADC counts as seen by the PMT/PIN Diode ratio for each position measured in a 10×10 array after the light has been mixed. In the plot, the first ten points correspond to the first row of ten fibers, the second ten points to the second row, etc. The top plot shows that the RMS difference from position to position is 1.3LED block were matched. In the bottom plot, mis–matched LEDs were used which resulted in a 2.4% RMS difference with maximum variations of 5.3%. From the figure, it is clear that matched LEDs improve light mixing.

Fig 17 shows a sampling of the ratio PMT/PIN at 9 different positions along the blank fiber block when the LED block is rotated 0-360 degrees in 90 degree increments. In each plot, a comparison is made of an LED block with matched LEDs and one with mismatched LEDs. The second plot confirms that the light is mixed by yielding the same amount of light at any orientation of the LED block. In addition, if the mismatched LED block exhibited a bright spot from one of the LEDs, it would have been clear in the Mixed LEDs points.

In conclusion, the LED block and two mixing blocks perform well the task of mixing the light. Mixing

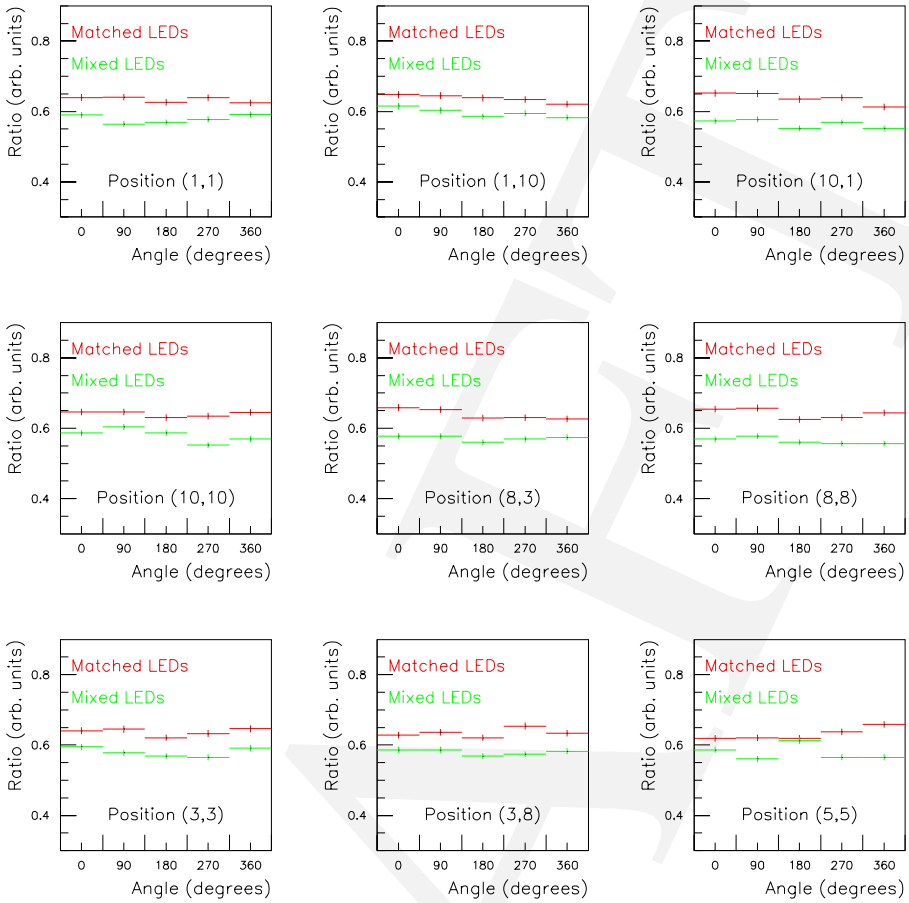

Figure 17: LED Block Rotations: Each plot is measured at a different position in the blank fiber block

is improved when the LEDs are matched within the LED block.

3.4 Light Distribution to PMTs

At this point along the light path from the LEDs to the PMTs, the light is mixed homogeneously, Sec. 3.3. The light is then distributed to the PMTs from the fibers in the fiber block. The concerns become:

- How consistently can the fibers be polished to transmit the light?
- How much light is lost at optical fiber couplers?
- How consistently can optical fiber couplers mate?
- How homogeneously can the light be distributed?

3.4.1 Fiber Polishing

A series of tests were performed to compare various fiber polishing techniques; details of the tests can be found in DØNote 3561[9]. The results have shown that the single fiber polishing machine, the Fiberfin III[10], performs as well as the previously preferred technique known as "ice polishing"; this was observed in both the visual comparison of polished surfaces and light transmission comparisons.

The modified Fiberfin III single fiber polisher was chosen since it would allow for the polishing of fibers with a previously installed HFBR-4501B simplex connectors. The advantages of polishing after the connectors are installed are: 1) the fiber surface is not damaged if mishandled when attaching the connector, and 2) the fiber surface is always flush with the connector end.

3.4.2 Tests on the Optical Fiber Coupling

Several tests were performed to determine the light transmission properties of the optical fiber couplers. In the tests, a pulsed LED was mounted in an cylindrical aluminum holder; into the other end of the holder, a fiber was attached so as to always be illuminated by the same surface of the LED.Another fiber was attached to a PIN diode/OpAmp circuit. On the ends of each fiber were Hewlett Packard HFBR-4501 simplex connectors. Coupling tests of the two fibers were performed with a Hewlett Packard HFBR-4505 bulkhead connector. Signals from the PIN diode were observed on a scope.

We used a setup with a LED pulser and a PIN diode/OpAmp circuit to try to improve the optical fiber coupler. For the different tests we tried a total of eight of the plastic bulkhead connectors, the two fibers attached to the circuit (simplex connector and bulkhead connector sides), and a total of five extra pieces of different lengths of fiber with their plastic end simplex connectors.

There are no significant differences in performance between gray and black bulkhead connectors and simplex connectors.

Light Loss in Optical Fiber Couplers

The couplers show a large sensitivity in the signal amplitude due to manipulations and perturbations of the simplex connectors within the bulkhead connectors. Using a coupler and by reinserting the connector into the bulkhead connector 40 times, we found that light transmission was reduced to 0.76 ± 0.04 of the original amplitude.

Transmission loss due to poor mating when fibers are retracted or protruding within the connectors is circumvented when using the single fiber polishing technique. The remaining loss is due to a missalignment of the two simplex connectors's axes within a bulkhead.

Several techniques were investigated to improve the alignment by increasing the tightness of the simplex connectors within the bulkhead connector. Ties around the bulkhead connector, stickers and several types of tapes around the ends of the simplex connector tips were tested. Most attempts made little improvement, and had some resulted in disadvantage, such as the tape not sticking well or leaving residues. The best solution was to put some Scotch Magic Tape around both simplex connectors.

Information from the manufacturer (3M) and our own observations, tells us that the Scotch Magic Tape lasts for very long time and preserves its characteristics well. We do not expect the backing or the adhesive to deteriorate after several years on the simplex connectors. Using the 19 mm wide tape from a standard tape dispenser, cut a 17 mm long piece, place the shorter side parallel to the axis of the connector and over the connector bump, and wrap it twice around to produce a double layer Repeat for the second simplex connector. Care should be taken to not to cover the end of the simplex connector, and to make sure that there are no wrinkles near the end. With the Magic Tape, the light transmission factor for the signal amplitude for a several simplex connectors and bulkhead connectors was measured to be 0.80 ± 0.015.

After many reconnections of the simplex connector, friction may peel off some of the tape. This is OK, as long as there still is at least one single layer left near the end of the simplex connector, and as long as little flakes don't cover the top of the simplex connector or the face of the fiber. If necessary, put a new piece of tape.

This system is quite stable under manipulation and perturbations, with two exceptions:

- The radius of curvature of the fiber must be > 15 cm near the connectors. If is less that 15 cm, a significant reduction in the signal amplitude is observed. A radius between 10 and 15 cm is

acceptable, as long as the curvature is far from the connectors. Putting ties around the connectors does not help.

- One cannot pull hard on the fiber, because there is the risk of loosening the fiber from the simplex connector and pulling back the face of the fiber away from the end of the simplex connector. This will leave an air gap between the two fibers. If this gap is greater than ∼0.3 mm, a 10%, or more, reduction of the signal is observed.

3.4.3 Light Distribution Results

Given that the light is well mixed up to the fiber block, Sec. 3.3, one can measure how homogeneously the fibers distribute the light to the PMTs.

To perform this measurement, a single pixel counter was used and operated at the nominal HV. A complete LMB was used in which each fiber was connected to the PMT. Simultaneous readings of the PMT output and PIN Diode output were recorded. The ratio of these results are plotted in Fig. 18.

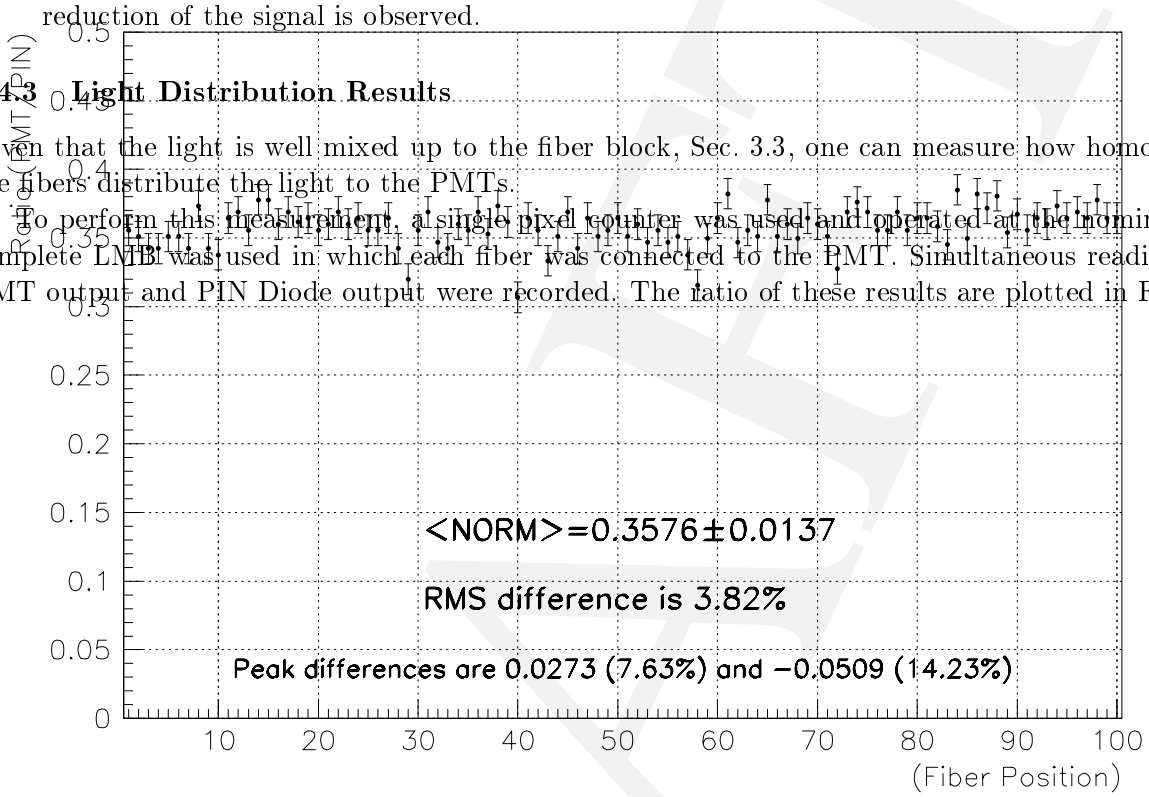

Figure 18: Light Distribution Uniformity: **TEST FIGURE FOR NOW**

3.5 LMB Stability

Fig. 19 shows the stability of the LED Pulser System over an 89 day period. During that period, individual runs of the muon test stand were taken which consisted of 16 separate measurements per run. The plot shows each measurement of each run in which a single counter was triggered by cosmic rays and LED triggers from the LED Pulser System. For each measurement of each run, ∼500 cosmic ray triggers and ∼1300 LED triggers were accumulated.

In Fig. 19, the top points (red) are the means of the ∼500 cosmic ray triggers for each measurement. The green points are the means of the ∼1300 event distributions when the counter was triggered by LED triggers. The LED Pulser System is designed to operate such that for each LED trigger, the PIN diode samples the light distributed to the PMTs. The blue points show the means of the distributions for the same LED triggers as the green, but as measured from the PIN diode. One can immediately see that the PIN diode tracks the PMT response to the LED triggers. The purple points—normalized so as to fit within the plot's scale—give the ratio of the PMT to PIN diode outputs. As described in Sec. 2.7, the ratio is used to remove any fluctuations in the LEDs. From the plot, one can see that the ratio tracks the PMT response as seen from the cosmic ray triggers over time.

Close scrutiny of the cosmic ray points in Fig. 19 shows a slight slope in the PMT response over the 3 month period. Fig. 20 shows the average each of the 16 measurements of each run replotted for both

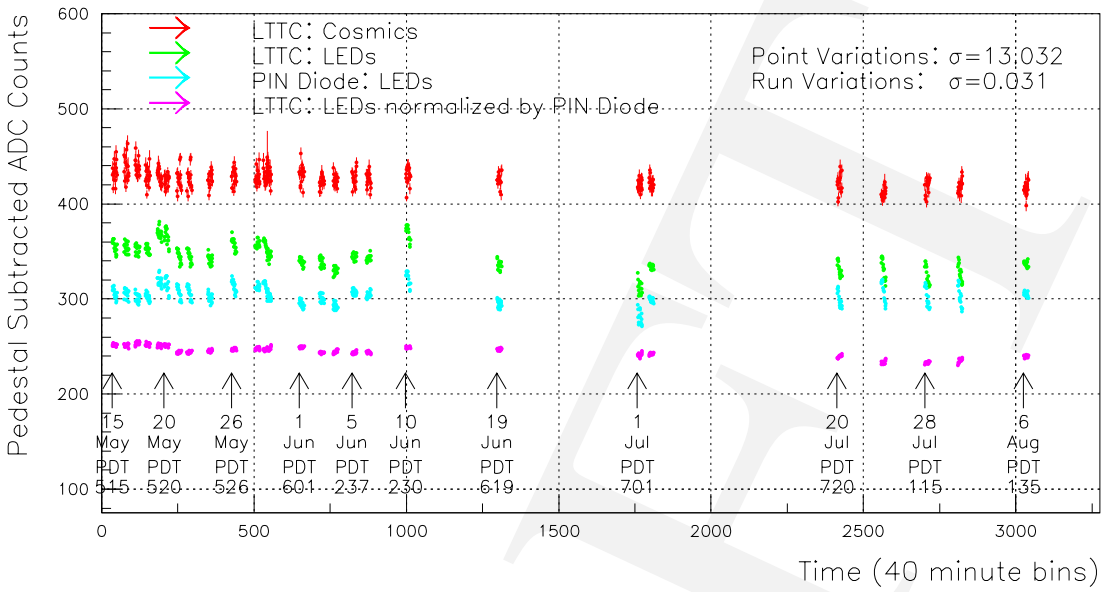

Figure 19: Long Term Stability Test of LED Pulser System

the cosmic ray triggers and the PMT/PIN ratio of LED triggers; the ratio points are normalized to fit the plot scale. Here the cosmic ray triggers are plotted in red, and a line is fit to the resulting points. The slope shows that the PMT's gain has dropped $\sim$3% over the course of the tests. The ratio points are plotted in blue, and a line is fit to these points. For comparison, the blue fit line is replotted as a dashed green line using the red line's y–intercept.

Analysis of the lines reveals a 4% drift in gain of the PMT. As can be seen in Fig. 20, a comparison with the slope of the ratio fit yields that the LED Pulser System tracks the PMT gain by $\sim$0.2% over the 3 month period.

The error bars on the ratio points in both Fig. 19 and Fig. 20 do not accurately represent the errors on the points. This is because both PMT and PIN diode measure light from the same source, and hence the errors are highly correlated; the error bars have been computed as uncorrelated errors. However, correcting the error bars does not change the fit result, only the χ^2 of the fit. Hence the errors are left in for comparison only.

The fit results show that the LED Pulser System will perform the task of monitoring the muon counter PMTs well within the specifications required.

3.6 PIN Diode Stability

3.7 System Stability Against Voltage Fluctuations

3.8 System Stability Against Temperature Fluctuations

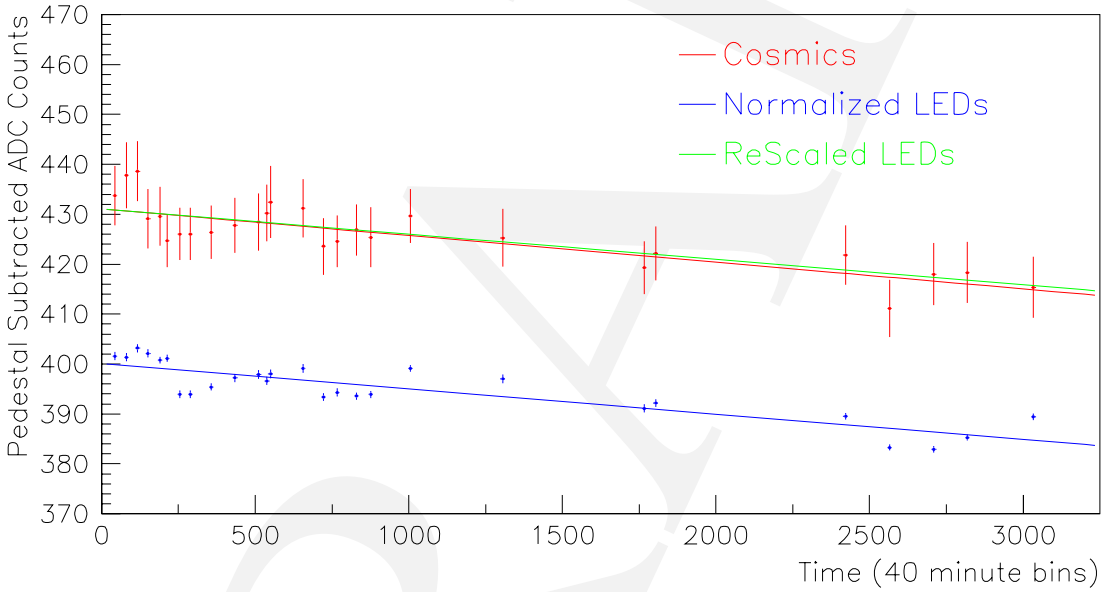

Figure 20: Replotting of the PMT gain drift

DRAFT

4 System Control

Communication with the SLP will be via VME commands generated by the 68k controller/crate master within the crate. Commands will consist of setting registers which control the DACs and Enable Registers within the SLP. The 68k controller will be addressed using the standard 1553 interface, or through the RS232 console port.

Tasks to be performed with the LED Pulser System may include:

- Test functionality of the PMTs
- Test for gain stability of the PMTs
- Test linearity of PMTs
- Scan gates
- Decouple front end electronics from PMTs by pulsing the system with no light to the PMTs

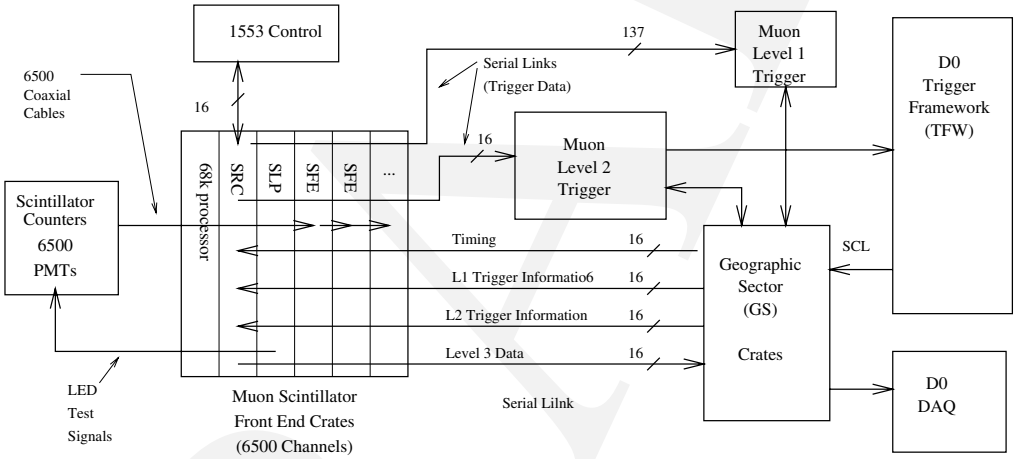

Figure 21: Driving circuit for single SLP channel

5 Component List and Cost Estimate

Tables 3 and 4 give counts for the number of major LED pulser system components for each scintillation counter detector region.

CMSC			
Part	Quantity	Unit Price	Total Price
LED Block	36	30.00	1,080.00
Upstream Mixing Block	36	40.00	1,440.00
Downstream Mixing Block	36	38.00	1,368.00
Fiber Block	36	50.00	1,800.00
Fiber (m)	6,486	0.55	3,567.30
Male Connectors	2,772	0.37	1,025.64
Bulkhead Connectors	1,326	0.55	729.30
PIN Diode	36	14.00	504.00
OpAmp Power +6V Supply	6	100.00	600.00
OpAmp Power -12V Supply	6	100.00	600.00
OpAmp Circuit Board	36	60.00	2,160.00
Power Connector	36	0.50	18.00
SLP	6	800.00	4,800.00
BNC Connectors	72	3.44	330.24
LED Circuit Board	36		900.00
Blue–Green LEDs	72	3.00	216.00
Base	36	50.00	1,800.00
Light Tight Cover	36	50.00	1,800.00
CMSC Total:			24,738.48

Table 3: Parts List and Cost Estimates for complete central system

DRAFT

FMSC			
Part	Quantity	Unit Price	Total Price
LED Block	48	30.00	1,440.00
Upstream Mixing Block	48	40.00	1,920.00
Downstream Mixing Block	48	38.00	1,824.00
Fiber Block	48	50.00	2,400.00
Fiber (m)	13,440	0.55	7,392.00
Male Connectors	9,408	0.37	3,480.96
Bulkhead Connectors	4,608	0.55	2,535.40
PIN Diode	48	14.00	672.00
OpAmp Power +6V Supply	12	100.00	1,200.00
OpAmp Power -12V Supply	12	100.00	1,200.00
OpAmp Circuit Board	48	60.00	2,880.00
Power Connector	48	0.50	24.00
SLP	12	800.00	9,600.00
BNC Connectors	96	3.44	330.24
LED Circuit Board	48	25.00	1,200.00
Blue LEDs	192	3.00	576.00
Base	48	50.00	2,400.00
Light Tight Cover	48	50.00	2,400.00
FMSC Total:			62,377.10

Table 4: Parts List and Cost Estimates for complete forward system

DRAFT

6 Manpower Requirements

A single fiber block requires ≈ 3 working days to construct, pot, and cure.

DRAFT

7 Production, Installation, and Commissioning

7.1 LMB Production

7.2 LMB Testing

7.3 LMB Installation and Fiber Routing

7.4 System Integration

DRAFT

8 Procurement and Schedule

Tab. 5 gives a time table for the LED Pulser System.

DRAFT

Who	Task Name	Duration	Start Date	End Date
PMH/ASI	Design/prototype CMSC calibration system	36w	10/1/96	5/24/97
PMH/ASI	Design/prototype FMSC calibration system	62w	11/1/96	6/30/98
PMH/DD	Procure FMSC fibers	2w	4/1/98	4/15/98
PMH/HTD	Procure CSMC fibers	3w	6/15/98	7/7/98
PMH/HTD	Procure fiber connectors	17w	4/15/98	8/15/98
PMH	Procure LEDs	3w	6/7/98	6/30/98
Student/PMH	Sort/test blue LEDs	5w	6/8/98	7/15/98
Student/PMH	Sort/test blue-green LEDs	6w	6/20/98	7/31/98
PMH	Procure parts for LMBs & fiber blocks	34w	10/1/97	6/1/98
LAB6	Machine LMBs	8w	6/7/98	8/7/98
JN?	Pot LED blocks	5w	7/1/98	8/7/98
LAB8	Machine fiber blocks	8w	1/2/98	3/2/98
	assemble fiber blocks	?w	?	?
JN	make 10x10 LMB prototye	6w	5/7/98	6/20/98
	make 7x7 LMB prototye	?w	?	?
JN	make 5x5 LMB prototye	40w	8/1/97	5/7/98
	make 4x4 LMB prototye	?w	?	?
DM	Modify existing CMSC-C counter for calibration	42w	6/25/97	6/15/98
PMH/ASI	Fabricate/test/install CMSC-C calibration system	16w	5/4/98	8/25/98
PMH/ASI	Install CMSC-A calibration system	?w	?	?
PMH/ASI	Install calib system on FMSC proto octant	1w	8/4/98	8/10/98
PMH/ASI	Install FMSC calibration system	54w	12/11/98	1/6/98
	Electronics			
TR	Fabricate/test SLP prototype	10w	5/14/98	7/24/98
TR	Layout SLP	1w	2/1/99	2/5/99
TR	Fabricate/test SLP	12w	2/8/99	4/30/99
TR/PMH/ASI	Prototype/test LDB	5w	5/15/98	6/22/98
TR	Fabricate LDB	7w	6/22/98	8/15/98
TR/PMH/ASI	Protoype/test PIN/OpAmp	36w	10/1/97	6/15/98
TR	Fabricate PIN/OpAmp	8w	6/15/98	8/15/98
	Constraints			
	(Assemble FMSC prototype octant)	4w	7/12/98	8/10/98
	(Install West CFB counters)	1w	8/17/98	8/21/98
	(Install 10% CMSCA counters and cables)	2w	9/9/98	9/22/98
	(Install EFB counters)	1w	10/21/98	10/27/98
	(Install Side B and Hole Counters)	2w	2/23/99	3/8/99
	(Assemble FMSC octants)	55w	12/4/98	1/6/00
	(Install East CFB counters)	1w	8/13/99	8/19/99
	(All FMSC octants assembled)	0w	12/3/99	12/3/99
	(Roll in)	8w	2/15/00	4/11/00
	(Cosmic Ray commissioning run)	8w	4/12/00	6/6/00

Table 5: Time table for design, fabrication, and testing of LED Pulser System. In paretheses are shown other components of muon upgrade schedule which impact or are impacted by LED Pulser System

DRAFT

9 Conclusion

In summary, we present an LED Pulser System which will be a powerful and essential tool for commissioning the muon scintillation counters to operating performance. During the run, it will give us simple means to quickly locate malfunctioning PMTs, and determine gain and timing drifts due to the PMTs.

DRAFT

References

[1] The E760 Collaboration, *The E760 Lead Glass Central Calorimeter: Design and Initial Test Results*, Nuclear Instruments and Methods A301, (1991) 47-60.

[2] J.M. Butler et al., *The DØ Muon Upgrade*, DØ Note 2780.

[3] B.S. Acharya et al., *Scintillation Counters for the DØ Muon Upgrade*, Nuclear Instruments and Methods A401, (1997) 45-62.

[4] A. Kholov, et al., *Muon System Electronics Upgrade*, DØ Note 3299.

[5] C. Rotolo and T. Fitzpatrick, *DØ Muon Scintillator Electronics Front End Module (SFE) Specification*, d0server1.fnal.gov/users/baldin/public/sfe_spec.pdf.

[6] C. Rotolo and T. Fitzpatrick, *DØ Muon Scintillator Electronics LED Pulser Module (SLP) Specification*, d0server1.fnal.gov/users/baldin/public/slp_spec.pdf.

[7] E.C. Dukes, *Monte Carlo Results on the Design of Light Guides for Scintillation Fiber Calorimeters*, Proceedings of the First International Conference on Calorimetry in High Energy Physics (1990), 177-188. DØNote 3299.

[8] Anton, G., K. Büchler, and M. Kückes, *Nuclear Instruments and Methods in Physics Research* A274 (1989) 222-226, North Holland, Amsterdam

[9] Hanlet, P., et al., *Comparison of Fiber Polishing Techniques*, DØ Note 3561.

[10] For more information or a demonstration of the Fiberfin III, contact PM MFG. Service, Inc., Ph. (630) 553-6924, Fax (630) 553-9025, website www.PM MFG.com, email PMMFG1.aol.com.

DRAFT